Carbon-13 NMR Spectroscopy, Electron Spin Distributions, and Valence State of Pentacoordinate Manganese Tetraphenylporphyrin Complexes

Peter Turner*,† and Maxwell J. Gunter*

Department of Chemistry, University of New England, Armidale, NSW, Australia 2351

*Received October 15, 1991**

The solution optical and NMR spectra of (TPP)MnX (X = F^-, NCO^-, $CH_3CO_2^-$, HCO_2^-, N_3^-, Cl^-, Br^-, NO_2^-, NO_3^-, NCS^-, CN^-, I^-, ClO_4^-, BF_4^-, $B(C_6H_5)_4^-$) indicate that ionic bonding may be particularly important in manganese tetraphenylporphyrin complexes. A Karplus–Fraenkel equation utilization of ^{13}C NMR spectra for the calculation of electron spin densities at the porphyrin nuclei uncovers an unexpectedly high positive π density at the pyrrole α-carbon sites. The densities for the acetato, nitrato, and perchlorato complexes are 0.049, 0.056, and 0.063, respectively. Such high densities are unlikely to be covalent in origin, and accordingly an axial ligand dependent mixture of the $[Mn^{II}(S = {}^3/_2, {}^4A_2)P(S = {}^1/_2, {}^2A_2)^{\bullet-}]^+ + [Mn^{III}(S = 2, {}^5A_1)P^{2-}]^+$ electronic states is proposed for the ground valence state of manganese tetraphenylporphyrin complexes. The calculations probably underestimate the α-carbon spin densities, so the C_{2v} $(d_{x^2-y^2})^0$ $(d_{z^2})^1$ $(d_{xz}\ d_{yz})^2$ $(d_{xy})^2$ $(a_2(\pi))^1$ $(a_1(\pi))^2$ $[Mn^{II}P^{\bullet-}]^+$ valence state is likely to be the principal ground-state contributor. The electron spin at the α-carbon sites dominates the carbon-13 spectroscopy through polarization and correlation. In contrast to previous deductions of negative $p(\pi)$ density, but in accord with the hyperporphyrin optical spectra, a high positive $p(\pi)$ density is present at the *meso* sites. This spin density is effectively undermined by the greater spin at the α-carbon location. The phenyl residue NMR reflects an axial ligand dependent balance of spin polarization and positive spin delocalization from the *meso* position. The carbon-13 spectra of the Br^-, Cl^-, and CN^- complexes indicate asymmetry in the porphyrin–phenyl residue interaction. The behavior of the axial ligand sensitive optical $\epsilon(III)/\epsilon(IV)$ ratio, suggests that the $a_2(\pi)$ orbital is the HOMO in manganese tetraphenylporphyrin complexes.

Introduction

Trivalent manganese complexes are implicated in a number of important biological processes.[1-10] It is generally accepted that Mn(III) is the preferred aerial oxidation state for manganese coordinated to a dianionic prophyrin ligand (P^{2-}) under ambient conditions. Synthetic manganese porphyrin complexes therefore offer useful platforms from which to explore the physical and chemical details of complex biological systems. Manganese porphyrin complexes have been used very successfully as models for lignase,[11,12] peroxidase,[13] the P-450 cytochromes,[14] and trans membrane electron-transfer agents.[15] Such complexes have also been used as NMR image enhancement agents,[16,17] nonlinear optical material,[18] and DNA binding and cleavage agents.[19,20] Water-soluble manganese porphyrins exhibit a cytotoxicity toward murine leukemia cells and a nuclease activity on DNA *in vitro*.[21] Patents have been lodged for the use of manganese porphyrins as DNA binding and cleavage agents, components of nonlinear optical devices, radiodiagnostic agents, foodstuff antioxidants, and P-450 mimics.

A large body of spectral, magnetic, and electrochemical evidence has accumulated in the literature in support of the $[Mn^{III}P^{2-}]^+$ valence formulation.[22-24] A convincing demonstration of the viability of the Mn(III) state in porphyrin complexes was provided in the far-infrared magnetic resonance study of iron and manganese porphyrin complexes reported by Brackett, Richards, and Caughey[25] in 1971. Although the $[Mn^{III}P^{2-}]^+$ valence formulation has an apparently irrefutable pedigree, Richert et al.[26] challenged this formulation in 1988. Anomalous electrochemical and X-ray absorption properties exhibited by a variety of manganese complexes, including manganese porphyrins, appear to be in conflict with the expectations of a Mn(III) state. Richert et al. suggested that the Mn(II) state is so favored by its symmetrical d^5 electronic manifold, that the Mn(III) state would not be supported by any organic ligand. Accordingly a manganese(II) porphyrin π cation radical valence formulation, $[Mn^{II}P^{\bullet-}]^+$, was proposed for manganese coordinated to a porphyrinic ligand. Such a valence state might explain the unusual

† Present address: Department of Inorganic Chemistry, School of Chemistry, University of Sydney, Sydney, NSW, Australia 2006.

* Abstract published in *Advance ACS Abstracts,* February 15, 1994.

(1) Weighardt, K. *Angew. Chem., Int. Ed. Engl.* **1989**, *28*, 1153.
(2) Renger, G. *Angew. Chem., Int. Ed. Engl.* **1987**, *26*, 643.
(3) Dismukes, G. C. *Photochem. Photobiol.* **1986**, *43*, 99.
(4) Dexheimer, S. L.; Klein, M. P. *J. Am. Chem. Soc.* **1992**, *114*, 2821.
(5) Livorness, J.; Smith, T. D. *Struct. Bonding* **1982**, *48*, 1.
(6) Yachandra, V. K.; Guiles, R. D.; McDermott, A. E.; Cole, J. L.; Britt, R. D.; Dexheimer, S. L.; Sauer, K.; Klein, M. P. *Biochemistry* **1987**, *26*, 5974.
(7) Fridovich, I. *Biochemistry* **1985**, *24*, 6460.
(8) *Superoxide and Superoxide Dismutases*; Michaelson, A. M., McCord, J. M., Fridovich, I., Eds.; Academic Press: New York, 1977.
(9) Ludwig, M. L.; Pattridge, K. A.; Stallings, W. C. In *Manganese in Metabolism and Enzyme Function*; Schramm, V. L., Wedler, F. C., Eds.; Academic Press: New York, 1986; pp 405–430.
(10) Willing, A.; Follman, H.; Auling, G. *Eur. J. Biochem.* **1988**, *170*, 603.
(11) Labat, G.; Meunier, B. *New. J. Chem.* **1989**, *13*, 801.
(12) Labat, G.; Meunier, B. *J. Org. Chem.* **1989**, *54*, 5008.
(13) Meunier, G.; de Montauzon, D.; Bernadou, J.; Grassy, G.; Bonnafous, M.; Cros, S.; Meunier, B. *Mol. Pharmacol.* **1988**, *33*, 93.
(14) Gunter, M. J.; Turner, P. *Coord. Chem. Rev.* **1991**, *108*, 115.
(15) Nango, M.; Mizusawa, A.; Miyake, T.; Yoshinga, J. *J. Am. Chem. Soc.* **1990**, *112*, 1640.
(16) MacMillan, J. H.; Cox, G. G.; Kimler, B. F.; Spicer, J. S.; Batnitzky, S. *Magn. Res. Imaging* **1991**, *9*, 553.
(17) Kellar, K. E.; Foster, N. *Inorg. Chem.* **1992**, *31*, 1353.
(18) Suslick, K. S.; Chen, C.-T.; Meredith, G. R.; Cheng, L.-T. *J. Am. Chem. Soc.* **1992**, *114*, 6928.
(19) Rodriguez, M.; Bard, A. J. *Inorg. Chem.* **1992**, *31*, 1129.
(20) Lu, M.; Guo, Q.; Pasternack, R. F.; Wink, D. J.; Seeman, N. C.; Kallenbach, N. R. *Biochemistry* **1990**, *29*, 1614.
(21) Ding, L.; Etemad-Moghadam, G.; Cros, S.; Auclair, C.; Meunier, B. *J. Chem. Soc., Chem. Commun.* **1989**, 1711.
(22) Boucher, L. J. *Coord. Chem. Rev.* **1972**, *7*, 289 and references cited therein.
(23) Chiswell, B.; McKenzie, E. D.; Lindoy, L. F. In *Comprehensive Coordination Chemistry*; Wilkinson, G., Gillard, R. D., McClevity, J. A., Eds.; Pergamon Press: Oxford, U.K., 1987; Vol. 4.
(24) Yamaguchi, K. S.; Sawyer, D. T. *Isr. J. Chem.* **1984**, *25*, 164.
(25) Brackett, G. C.; Richards, P. L.; Caughey, W. S. *J. Chem. Phys.* **1971**, *54*, 4383.
(26) Richert, S. A.; Tsang, P. K. S.; Sawyer, D. T. *Inorg. Chem.* **1988**, *27*, 1814.

0020-1669/94/1333-1406$04.50/0

manganese porphyrin electrochemical and axial ligand binding properties, described by Kelly and Kadish[27] in 1982.

The use of NMR spectroscopy as a sensitive probe of spin distribution in metalloporphyrin complexes is well established.[28-31] Optical spectroscopy has been used to identify the metal oxidation state in manganese porphyrin complexes.[32,33] Additionally, the optical and NMR spectra of several manganese(III) porphyrin π cation radicals have now been described in the literature.[34-37] In conjunction with the well-understood orbital structure of the porphyrin ligand (*vide infra*), optical and NMR spectroscopies may be used to map axial ligand dependent variations in charge donation from the porphyrin to the metal ion and concomitant changes in spin transfer from the metal ion to the porphyrin. A combination of optical and NMR spectroscopies should therefore constitute an effective probe of manganese porphyrin covalency and valence-state structure. In the application of this probe, the Richert et al. proposal may be tested.

As a convenience, solution complex formulations are enclosed in brackets to distinguish them from solid formulations; for example [(TPP)Mn(ClO_4)] is the solution formulation for (TPP)Mn(H_2O)$_2ClO_4$ dissolved in methylene chloride. Although there are crystal structures demonstrating that methylene chloride can act as a ligand,[38,39] the evidence presented in the literature[22] shows that it is too weak a ligand to have any significant impact on the chemical and physical properties of manganese porphyrin complexes.

Experimental Details

Instrumentation. Infrared spectra were recorded on a Perkin-Elmer 1725X FT-IR machine, and electronic spectra were measured with a Hitachi U3200 spectrophotometer or a Hewlett Packard 8452A diode array machine. The proton and carbon-13 NMR spectra were recorded on a Bruker AC 300 spectrometer, and X-band EPR spectra were kindly recorded by Dr. K. S. Murray of Monash University, Melbourne, Australia.

Materials. Reagent grade toluene and benzene were repeatedly washed with concentrated sulfuric acid, until the aqueous layer became colorless, and then washed with water, dilute sodium bicarbonate, and water again and finally dried over calcium chloride to be distilled onto activated molecular sieves. All chlorinated solvents were stirred over potassium carbonate, distilled, and kept for no longer than 1 week before redistilling. Analytical alkanes were dried over activated sieves. The complexes were prepared by standard procedures,[40,41] and we have obtained crystal structures for most of the complexes that have not previously been reported.[42,43] Elemental analyses were undertaken by the Micro-Analytical Unit of the Research School of Chemistry at the Australian National University.

(TPP)Mn(H_2O)$_2BF_4$ was prepared in the same manner[41] as (TPP)-Mn(H_2O_2)ClO_4, with 10% HBF_4 being substituted for 10% $HClO_4$. The complex was recrystallized overnight, following dissolution in toluene and immediate filtration. The crystalline material was analyzed for (TPP)Mn(H_2O)$_2BF_4$·H_2O as $C_{44}H_{34}N_4O_3BF_4Mn$. Anal. Calcd: C, 65.34; H, 4.2; N, 6.92. Found: C, 65.58; H, 3.93; N, 6.89. Considerable difficulty was encountered in preparing this complex reproducibly, and the monitoring of spectroscopic solutions revealed some instability; the decomposition product has not been identified. Such problems with the BF_4^- counterion in metalloporphyrin complexes have been noted in the literature.[44,45]

(TPP)Mn(H_2O)$_2B(C_6H_5)_4$ was prepared by dissolving 10 mg of (TPP)Mn(H_2O)$_2ClO_4$ in 2 mL of acetonitrile, adding 20 equiv of NaB-(C_6H_5)$_4$ dissolved in an equal volume of acetonitrile, and then carefully adding water dropwise. The resulting crystalline material was treated in the same fashion. The product was analyzed for (TPP)Mn(H_2O)$_2$B-(C_6H_5)$_4$ as $C_{68}H_{52}N_4BO_2Mn$. Anal. Calcd (found): C, 79.84 (80.26); H, 5.12 (5.10); N, 5.79 (5.44). Replacing acetonitrile with DMF produces (TPP)Mn(DMF)$_2B(C_6H_5)_4$.

Results and Discussion

Optical and Proton NMR Spectroscopy. The porphyrin orbital and electronic structure has been explored with increasing sophistication for more than 40 years.[46-89] In traditional D_{4h} terms, Figure 1 depicts the lobes of the doubly degenerate $e_g(\pi^*)$

(27) Kelly, S. L.; Kadish, K. M. *Inorg. Chem.* **1982**, *21*, 3631.
(28) La Mar, G. N.; Walker (Jensen), F. A. *The Porphyrins*; Academic Press: New York, 1979; Vol. IV.
(29) La Mar, G. N.; Walker, F. A. *J. Am. Chem. Soc.* **1975**, *97*, 5103.
(30) Goff, H. M.; Hansen, A. P. *Inorg. Chem.* **1984**, *23*, 321.
(31) Bertini, I.; Luchinat, C. *NMR of Paramagnetic Molecules in Biological Systems*; Benjamin/Cummings: Menlo Park, CA, 1986, pp 249.
(32) Williamson, M. M.; Hill, C. L. *Inorg. Chem.* **1986**, *25*, 4668.
(33) Arasasingham, R. D.; Bruice, R. D. *Inorg. Chem.* **1990**, *29*, 1422.
(34) Goff, H. M.; Phillippi, M. A.; Boersma, A. D.; Hansen, A. P. *Adv. Chem. Ser.* **1982**, *No. 201*, 357.
(35) Spreer, L. O.; Maliyackel, A. C.; Holbrook, S.; Otvos, J. W.; Calvin, M. *J. Am. Chem. Soc.* **1986**, *108*, 4133.
(36) Carnieri, N.; Harriman, A.; Porter, G.; Kalyanasundraram, K. *J. Chem. Soc., Dalton Trans.* **1982**, 1231.
(37) Maliyackel, A. C.; Otvos, J. W.; Calvin, M.; Spreer, L. O. *Inorg. Chem.* **1987**, *26*, 4133.
(38) Newbound, T. D.; Colsman, M. R.; Miller, M. M.; Wulfsberg, G. P.; Andersen, O. P.; Strauss, S. H. *J. Am. Chem. Soc.* **1989**, *111*, 3762.
(39) Brown, M.; Waters, J. M. *J. Am. Chem. Soc.* **1990**, *112*, 2442.
(40) Powell, M. F.; Pai, E. F.; Bruice, T. C. *J. Am. Chem. Soc.* **1984**, *106*, 3277.
(41) Kennedy, B. J.; Murray, K. S. *Inorg. Chem.* **1985**, *24*, 1557.
(42) Turner, P.; Gunter, M. J.; Hambley, T. W.; White, A. H.; Skelton, B. W. *Inorg. Chem.* **1992**, *31*, 2295.
(43) Turner, P.; Gunter, M. J.; Skelton, B. W.; Wen, H.; White, A. H. Submitted for publication in *Inorg. Chem.*
(44) Cohen, I. A.; Summerville, D. A.; Su, S. R. *J. Am. Chem. Soc.* **1976**, *98*, 5813.
(45) Reed, C. A.; Mashiko, T.; Bently, S. P.; Kastner, M. E.; Scheidt, W. R.; Spartalian, K.; Lang, G. *J. Am. Chem. Soc.* **1979**, *101*, 2948.
(46) Longuet-Higgins, H. C.; Rector, C. W.; Platt, J. R. *J. Chem. Phys.* **1950**, *18*, 1174.
(47) Gouterman, M. *J. Chem. Phys.* **1959**, *30*, 1139.
(48) Kobayashi, H.; Yanagawa, Y.; Osada, H.; Minami, S.; Shimizu, M. *Bull. Chem. Soc. Jpn.* **1973**, *46*, 1471.
(49) Maggiora, G. M. *J. Am. Chem. Soc.* **1973**, *95*, 6555.
(50) Fajer, J.; Borg, D. C.; Forman, A.; Dolphin, D.; Felton, R. H. *J. Am. Chem. Soc.* **1970**, *92*, 3451.
(51) Gouterman, M.; Hanson, K. H.; Khalil, G. E.; Leenstra, W. R.; Bouchler, J. W. *J. Phys. Chem.* **1975**, *62*, 2343.
(52) Spangler, D.; Maggiora, G. M.; Shipman, L. L.; Christoffersen, R. E. *J. Am. Chem. Soc.* **1977**, *99*, 7478.
(53) Gouterman, M. In *The Pophyrins*; Dolphin, D., Ed.; Academic Press: New York, 1979; Vol. III.
(54) Hanson, L. K. *Int. J. Quantum Chem.* **1979**, *6*, 73.
(55) Hanson, L. K.; Hoffman, B. M. *J. Am. Chem. Soc.* **1980**, *102*, 4602.
(56) Mishra, S.; Chang, J. C.; Das, T. P. *J. Am. Chem. Soc.* **1980**, *102*, 2675.
(57) Spellane, P. J.; Gouterman, M.; Antipas, A.; Kim, S.; Liu, Y. C. *Inorg. Chem.* **1980**, *19*, 386.
(58) Berkovitch-Yellin, Z.; Ellis, D. E. *J. Am. Chem. Soc.* **1981**, *103*, 6066.
(59) Hanson, L. K.; Chang, C. K.; Davis, M. S.; Fajer, J. *J. Am. Chem. Soc.* **1981**, *103*, 663.
(60) Kashiwagi, H.; Obara, S. *Int. J. Quantum Chem.* **1981**, *20*, 843.
(61) Mun, S. K.; Mallick, M. K.; Mishra, S.; Chang, J. C.; Das, T. P. *J. Am. Chem. Soc.* **1981**, *103*, 5024.
(62) Dedieu, A.; Rohmer, M.-M.; Veilard, A. *Adv. Quantum Chem.* **1982**, *16*, 43.
(63) Lee, L. K.; Sabelll, N. H.; LeBreton, P. R. *J. Phys. Chem.* **1982**, *86*, 3926.
(64) Fujita, I.; Hanson, L. K.; Walker, F. A.; Fajer, J. *J. Am. Chem. Soc.* **1983**, *105*, 3296.
(65) Shelnutt, J. A.; Straub, K. D.; Rentzepis, P. M.; Gouterman, M.; Davidson, E. R. *Biochemistry* **1984**, *23*, 3946.
(66) Shelnutt, J. A. *J. Phys. Chem.* **1984**, *88*, 6121.
(67) Shelnutt, J. A. *J. Phys. Chem.* **1984**, *88*, 4988.
(68) Newton, J. E.; Hall, M. B. *Inorg. Chem.* **1985**, *24*, 2573.
(69) Rawlings, D. C.; Gouterman, M.; Davidson, E. R.; Feller, D. *Int. J. Quantum Chem.* **1985**, *28*, 823.
(70) Saito, M.; Kashiwagi, H. *J. Chem. Phys.* **1985**, *82*, 848.
(71) Shelnutt, J. A.; Ortiz, V. *J. Phys. Chem.* **1985**, *89*, 4733.
(72) Edwards, W. D.; Weiner, B.; Zerner, M. *J. Am. Chem. Soc.* **1986**, *108*, 2196.
(73) Lecomte, C.; Blessing, R. H.; Coppens, P.; Tabard, A. *J. Am. Chem. Soc.* **1986**, *28*, 4574.
(74) Loew, G. H.; Collins, J.; Like, B.; Waleh, A.; Pudzianowski, A. *Enzyme* **1986**, *36*, 54.
(75) Masthay, M. B.; Finsden, L. A.; Pierce, B. M.; Bocian, D. F.; Lindsey, J. S.; Birge, R. R. *J. Chem. Phys.* **1986**, *84*, 3901.
(76) Nagashima, U.; Takada, T.; Ohno, K. *J. Chem. Phys.* **1986**, *85*, 4524.
(77) Sekino, H.; Kobayashi, H. *J. Chem. Phys.* **1987**, *86*, 5045.
(78) VanAtta, R. B.; Strouse, C. E.; Hanson, L. K.; Valentine, J. S. *J. Am. Chem. Soc.* **1987**, *109*, 1425.
(79) Barkigia, K. M.; Chantranupong, L.; Smith, K. M.; Fajer, J. *J. Am. Chem. Soc.* **1988**, *110*, 7566.
(80) den Boer, D. H. W.; van Lenthe, J. H.; van der Made, A. H. *Recl. Trav. Chim. Pays-Bas* **1988**, *107*, 256.

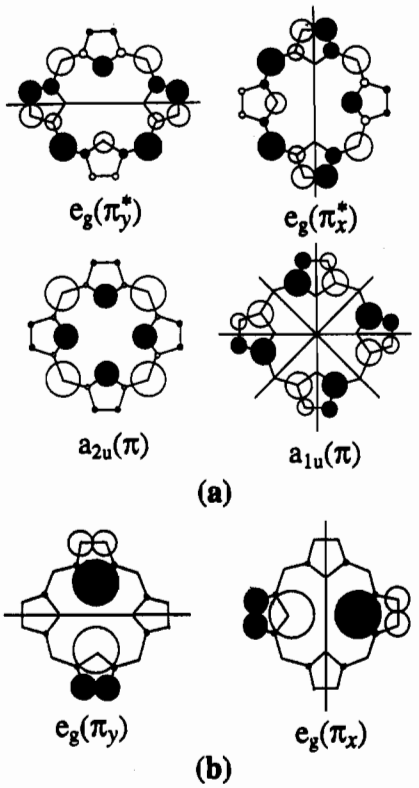

Figure 1. More important porphyrin molecular orbitals: (a) HOMO and LUMO set (Binstead, R. A.; Crossley, M. J.; Hush, N. S. *Inorg. Chem.* **1991**, *30*, 1259); (b) lower lying filled $e_g(\pi)$ orbital diagram (La Mar, G. N.; Walker, F. A. In *The Porphyrins*; Dolphin, D., Ed.; Academic Press: New York, 1979; Vol. IV, Chapter 2).

LUMO pair and the accidentally degenerate $a_{2u}(\pi)$ and $a_{1u}(\pi)$ HOMO pair. There is a large gap[77] of around 3 eV between the HOMO pair and the next highest occupied $b_{1g}(n)$ nitrogen-based "lone-pair" HOMO-1. Just below the HOMO-1 is the important (*vide infra*) $e_g(\pi)$ HOMO-2 pair. Actually, the precise ordering of orbitals below the HOMO level appears to be sensitive to the applied computational technique[49,62,63,77] and may not become fixed until basis sets appropriate to the porphyrin macrocycle are implemented.[86] Pentacoordinate metalloporphyrins have a *sad* core conformation[43,90,91] that is better described by C_{2v} symmetry; however, the deviation from planarity is not severe and so should not seriously alter the topology of the D_{4h}-determined orbitals. In C_{2v} terms, the LUMOs are labeled $b_1(\pi^*)$ and $b_2(\pi^*)$, $b_{1g}(n)$ becomes $a_1(n)$, and symmetry across a vertical mirror means that the $a_{2u}(\pi)$ HOMO becomes $a_1(\pi)$, whereas the $a_{1u}(\pi)$ HOMO changes to $a_2(\pi)$ (Figure 2).

Were the macrocycle of a (TPP)Mn(X) complex to be strictly planar, then covalent charge donation from the $a_1(\pi)$ HOMO to the metal $a_1(3d_{z^2})$ orbital and from the $a_2(\pi)$ HOMO to the $a_2(3d_{xy})$ orbital would be severely restricted by a lack of orbital

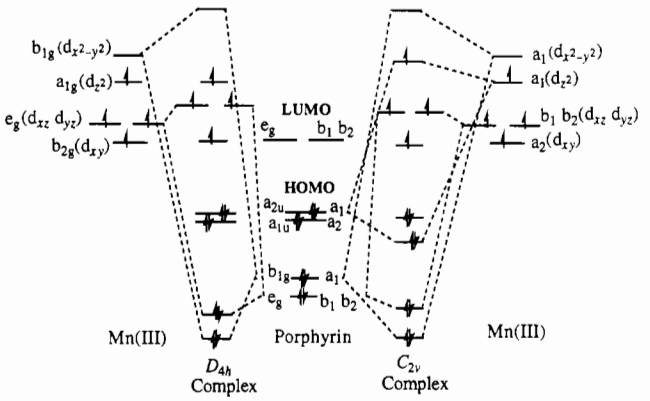

Figure 2. Qualitative comparison of spin delocalization in D_{4h} and C_{2v} symmetry. Lowering the symmetry results in σ spin transfer into an orbital having a degree of porphyrin $a_1(\pi)$ HOMO character (see also Figure 1). Axial ligand interactions and metal orbital interactions with the porphyrin LUMO set are not included in this diagram.

overlap. However, a displaced metal ion and *sad* core conformation would support some a_1 orbital overlap, whereas a slight improvement in the orbital phase relationship is unlikely to result in any significant overlap between the $a_2(\pi)$ HOMO and $a_2(3d_{xy})$ orbitals, because they are spatially too far apart. Most of the covalent charge compensation is likely to come from π bonding between the porphyrin and metal $b_1(\pi)$ and $b_2(\pi)$ orbitals and σ bonding between the porphyrin $a_1(n)$ and metal $a_1(3d_{x^2-y^2})$ orbitals. The latter orbital mixing may prevent $a_1(\pi)$ access to the $a_1(3d_{x^2-y^2})$ orbital.

NMR spectroscopy provides a sensitive probe of metal to porphyrin spin distribution and hence covalent interaction. La Mar and Walker[29,92] have demonstrated that the minimal magnetic anisotropy and small zero-field splitting of a porphyrin coordinated manganese(III) ion ensures that the isotope shifts and resonance broadening in the proton NMR spectrum arise almost entirely from "through bond" contact interactions. Unusually, the 3d valence orbitals of Mn(III) are approximately degenerate with the LUMO level of the porphyrin dianion macrocycle,[48,51,53] which is about 6 eV above the HOMO level.[77] Consequently the β-pyrrole proton resonance reflects not only the level of π charge donation from the porphyrin $b_1(\pi)$ and $b_2(\pi)$ to the metal $b_1(3d_{xz})$ and $b_2(3d_{yz})$ orbitals but also the extent of mixing between the porphyrin LUMO pair and the metal d_{xz} and d_{yz} orbitals (back-bonding). The greater the level of π spin transfer to the β-pyrrole carbon position, the larger the upfield (positive) β-pyrrole proton isotropic shift.

The 30-year-old Gouterman four-orbital model[47,53] continues to provide an excellent first-order account of porphyrin and metalloporphyrin optical spectra.[48,51,53,57,65-67,71,77,82,85] The four-orbital model does not explain all porphyrin optical features; other orbital transitions and double-photon absorption have been shown[63,75,76,89,93] to make contributions to porphyrin spectroscopy. Of particular relevance to this discussion, the band V wavelength and the $\epsilon(V)/\epsilon(VI)$ ratio of d-hyperporphyrin optical spectra provide a direct indication of the axial ligand sensitive disposition of the metal $3d_{xz}$ and $3d_{yz}$ orbitals with respect to the porphyrin LUMO level[53,63,75,76,89,93] (see Figure 3 for band labeling). When the ratio is greater than one, the metal orbitals reside above the porphyrin LUMO pair. This informative spectral property is the result of a configuration interaction between the porphyrin HOMO–LUMO transition and the HOMO to metal charge-transfer transition (B-CT CI). Additionally, a CI between the components of the accidentally doubly degenerate HOMO–LUMO transition (B-Q CI) has the useful consequence that the

(81) Axe, F. U.; Flowers, C.; Loew, G. H.; Waleh, A. *J. Am. Chem. Soc.* **1989**, *111*, 7333.
(82) Orti, F.; Brédas, J. L. *Chem. Phys. Lett.* **1989**, *164*, 247.
(83) Rhomer, M.-M. *Inorg. Chem.* **1989**, *28*, 4574.
(84) Barkigia, K. M.; Berber, D. M.; Fajer, J.; Medforth, C. J.; Renner, M. W.; Smith, K. M. *J. Am. Chem. Soc.* **1990**, *112*, 8851.
(85) Binstead, R. A.; Crossley, M. J.; Hush, N. S. *Inorg. Chem.* **1990**, *30*, 1259.
(86) Ghosh, A.; Almlöf, J.; Gassman, P. G. *Chem. Phys. Lett.* **1991**, *186*, 113.
(87) Loew, G. H.; Axe, F. U.; Collins, J. R.; Du, P. *Inorg. Chem.* **1991**, *30*, 2297.
(88) Prendergast, K.; Spiro, T. G. *J. Phys. Chem.* **1991**, *95*, 9728.
(89) Foresman, J. B.; Head-Gordon, M.; Pople, J. A. *J. Phys. Chem.* **1992**, *96*, 135.
(90) Scheidt, W. R.; Lee, Y. J. *Struct. Bond.* **1987**, *64*, 1557.
(91) Munro, O. Q.; Bradley, J. C.; Hancock, R. D.; Marques, H. M.; Marsicano, F.; Wade, P. W. *J. Am. Chem. Soc.* **1992**, *114*, 7218.
(92) La Mar, G. N.; Walker, F. A. *J. Am. Chem. Soc.* **1973**, *95*, 6950.
(93) Rende, D. E.; Heagy, M. D.; Heuer, W. B.; Liou, K.; Thompson, J. A.; Hoffman, B. M.; Musselman, R. L. *Inorg. Chem.* **1992**, *31*, 352.

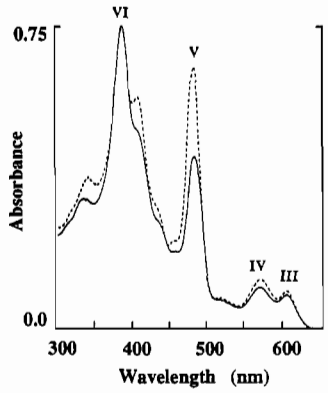

Figure 3. Optical spectrum of (TPP)Mn(H_2O)$_2$$ClO_4$ in dichloromethane at 1.15×10^{-5} M (solid line) and toluene at 1.15×10^{-5} M (dashed line). In CH_2Cl_2, the spectrum is very similar to that of [(TPP)Mn(Cl)]ClO_4, a Mn(III) porphyrin π radical cation complex. Band V gains intensity in the aromatic solvent.

Table 1. Proton NMR Features for (TPP)Mn(X) in CD_2Cl_2[a]

X	phenyl *ortho*	phenyl *meta*	phenyl *para*	β-pyrrole
F^-	*b*	8.15 (–0.4)	7.3 (0.45)	–19.7 (28.55)
NCO^-	*b*	8.3 (–0.55)	7.2 (0.55)	–21.5 (30.35)
$CH_3CO_2^-$	*b*	8.25 (–0.5)	7.3 (0.45)	–21.8 (30.65)
N_3^-	*b*	8.4 (–0.65)	7.3 (0.45)	–22.1 (30.95)
Cl^-	*b*	8.3 (–0.55)	7.3 (0.45)	–22.3 (31.15)
Br^-	*b*	8.45 (–0.7)	7.5 (0.25)	–23.5 (32.35)
HCO_2^- [d]	*b*	8.2 (–0.45)	7.35 (0.4)	–25.7 (34.55)
I^-	9.2[c] (–1.0)	8.55 (–0.8)	7.75 (0.0)	–25.9 (34.75)
NCS^-	*b*	8.3 (–0.55)	7.3 (0.45)	–26.6 (35.45)
NO_2^-	*b*	8.15 (–0.4)	7.4 (0.35)	–27.3 (36.15)
NO_3^-	*b*	8.2 (–0.45)	7.45 (0.3)	–28.0 (36.85)
CN^-	*b*	8.2 (–0.45)	7.2 (0.55)	–28.5 (37.35)
ClO_4^-	9.0 (–0.8)	7.9 (–0.15)	7.7 (0.05)	–36.0 (44.85)
BF_4^- [d]	9.0[c] (–0.8)	8.0 (–0.25)	7.7 (0.05)	–36.4 (45.25)

[a] At 25 °C and referenced against TMS in ppm; isotropic shifts with respect to (TPP)Zn are given in parentheses (+ is upfield). [b] Not observed; under *m* and *p* bands. [c] Unresolved shoulder on *m* peak. [d] In $CDCl_3$.

ϵ(III)/ϵ(IV) ratio can reveal the extent of any deviation from degeneracy of the HOMO level $a_1(\pi)$ and $a_2(\pi)$ orbitals.[57,85,94]

The proton NMR spectra of a variety of (TPP)Mn(X) complexes dissolved in CD_2Cl_2 at 25 °C are summarized in Table 1, and Table 2 contains the principal optical absorption features of these complexes in CH_2Cl_2. In general the zero field splitting parameter is probably the best overall indicator of axial ligand field strength, and NMR spectroscopy has been used to so determine relative axial ligand field strengths in high-spin Fe(III) porphyrin complexes.[102] This approach is not possible for manganese tetraphenylporphyrin complexes, because the minimal magnetic anisotropy prevents a clear distinction between dipolar and contact effects at any proton site on the TPP ligand (*vide infra*). Solid-state magnetic measurements of *D* are needed. The axial ligand field is a composite property determined by the ligands σ and π donor-acceptor capacity, hardness or softness (HOMO–LUMO separation[95]), and electrostatic field. The β-pyrrole proton resonance and the band V and VI wavelengths and intensity ratios should be particularly sensitive to π interactions between the porphyrin complex and the attendant axial ligand. Yet the correlation between these Table 1 and 2 parameters and the spectrochemical series, π bases < weak π bases < no π interaction < π acids, is rather weak. The spectrochemical series would suggest that the β-pyrrole proton isotropic shifts should increase in the order $I^- < Br^- < Cl^- < NO_3^- < F^- < NCS^- < NO_2^- < CN^-$, rather than $F^- < Cl^- < Br^- < I^- < NCS^- < NO_2^- < NO_3^- < CN^-$.

The distinction between the β-pyrrole proton isotropic shift series of Table 1 and the spectrochemical series seems to emphasize the role of the axial crystal field (its strength and polarizability) in influencing the level of π interaction between the metal and the porphyrin. If so, then ionic bonding must be of some importance in manganese tetraphenylporphyrin complexes. This possibility was first suggested 20 years ago by Boucher,[22] in a review of manganese porphyrin optical spectroscopy. The fast neutral ligand exchange observed for manganese porphyrins,[30,96,97] but not iron porphyrins,[98,99] provides further support for this proposition. The valence orbitals of Fe(III) are lower in energy[51,53] and so more covalently accessible than those of Mn(III). It may be then, that axial ligand binding to the formally hard manganese Lewis acid is, in Klopman's terms,[100,101] predominantly charge rather than orbital controlled in porphyrin complexes.

There should be a strong correlation between the B-CT CI dependent parameters of Table 2 (i.e. the band V and VI wavelengths and intensity ratios) and the β-pyrrole proton isotropic shifts of Table 1, because both depend on the energy of the metal d_{xz} and d_{yz} orbitals. The lack of such a correlation presumably reflects the complexity of excited-state processes and interactions. Porphyrin orbital contractions associated with covalent charge donation may influence the B-Q and B-CT CI, and excited-state electronic interactions will depend on the polarizability of the axial ligand.

The β-pyrrole proton NMR resonance and the ϵ(III)/ϵ(IV) ratio provide complementary views of the dependence of the porphyrin to metal covalency on the nature of the axial ligand. The axial ligand orbitals will have a greater impact on the metal d_{xz}, d_{yz}, and d_{z^2} metal orbitals than on the d_{xy} and $d_{x^2-y^2}$ orbitals. Any energetic promotion of the d_{xz} and d_{yz} orbitals away from the porphyrin HOMO and LUMO level will reduce the π spin density at the β-pyrrole position, while raising the d_{z^2} orbital energy will lower the level of σ spin transfer to the ligand. The data in Table 2 are ordered with respect to the ϵ(III)/ϵ(IV) ratio. A rising optical ϵ(III)/ϵ(IV) ratio signals a decline of the HOMO level degeneracy and, given that the $a_1(\pi)$ orbital is a much more competent covalent donor than the $a_2(\pi)$ orbital, thus presumably provides an indicator of σ charge donation from the $a_1(\pi)$ orbital to the metal $a_1(3d_{z^2})$ orbital (leaving the $a_2(\pi)$ orbital as the HOMO). The pattern of the axial ligand dependence of the ϵ(III)/ϵ(IV) ratio suggests that this ratio is particularly sensitive to the hardness of the axial ligand field and the size of the coordinating atom. In fact there appears to be a simple distinction between hard and soft ligands, with ligands having ϵ(III)/ϵ(IV) < 1 being hard. Apparently the crystal field of a hard axial ligand elevates the metal d_{z^2} orbital and so restricts porphyrin σ donation into this orbital.

Axial ligands with acceptor capacity, such as the azido and cyano ligands, may further encourage σ donation from the porphyrin. Although σ spin attenuates rapidly with distance, its transfer to the phenyl residues via the *meso* lobe of the $a_1(\pi)$ orbital probably makes a contribution to the increasingly downfield bias in the *meta*- and *para*-phenyl proton NMR shifts, as X is varied from F to I. A likely additional contribution to this bias is a change in the magnetic anisotropy from being slightly axial to being slightly equatorial (*vide infra*). Noteworthy is the strong correlation between the *meta*- and *para*-phenyl proton shifts and the ϵ(III)/ϵ(IV) ratio of the halide complexes in particular.

(94) VanCott, T. C.; Rose, J. L.; Misener, G. C.; Williamson, B. E.; Schrimpf, A. E.; Boyle, M. E.; Schatz, P. N. *J. Phys. Chem.* **1989**, *93*, 2999.
(95) Pearson, R. G. *Inorg. Chem.* **1988**, *27*, 734.
(96) Hill, C. L.; Williamson, M. M. *Inorg. Chem.* **1985**, *24*, 2836.
(97) Turner, P.; Gunter, M. J.; Skelton, B. W.; Wen, H.; White, A. H.; Hambley, T. W. Manuscript in preparation.
(98) Satterlee, J. D.; La Mar, G. N.; Frye, J. S. *J. Am. Chem. Soc.* **1976**, *98*, 7275.
(99) Satterlee, J. D.; La Mar, G. N.; Bold, T. J. *J. Am. Chem. Soc.* **1977**, *99*, 1088.
(100) Dronowski, R. *J. Am. Chem. Soc.* **1992**, *114*, 7230.
(101) Klopman, G. *J. Am. Chem. Soc.* **1968**, *90*, 223.
(102) Goff, H. M.; Shimomura, E. T.; Phillippi, M. A. *Inorg. Chem.* **1983**, *22*, 66.

Table 2. Room-Temperature Optical Features for (TPP)Mn(X) at Approximately 10^{-4} M in CH_2Cl_2

	band VI		band V		band IV		band III					
X⁻	λ (nm)	ϵ^a	λ (nm)	ϵ^a	λ (nm)	ϵ^a	λ (nm)	ϵ^a	$\epsilon(V)+\epsilon(VI)^a$	$\Delta\lambda$(V–VI)	$\epsilon(V)/\epsilon(VI)$	$\epsilon(III)/\epsilon(IV)$
F^-	366[b]	*c*	457	*c*	572	*c*	606	*c*	*c*	91	4.16	0.82
ClO_4^-	390	6.54	486	3.91	571	0.98	606	0.82	10.5	96	0.59	0.84
NO_3^-[d]	384	4.40	478	8.10	577	0.87	611	0.74	12.5	94	1.84	0.85
BF_4^-	389	*c*	482	*c*	569	*c*	604	*c*	*c*	93	0.51	0.85
NO_3^-	387	5.00	480	6.10	575	0.97	609	0.85	11.1	93	1.22	0.88
$CH_3CO_2^-$	372	4.54	470	11.7	577	0.96	612	0.92	16.2	98	2.58	0.96
HCO_2^-	376	*c*	472	*c*	577	*c*	611	*c*	*c*	96	2.52	0.98
NO_2^-	381	4.79	477	8.09	580	0.79	615	0.81	12.9	96	1.69	1.03
NCO^-	375	4.90	475	11.04	583	0.92	617	1.05	15.9	100	2.25	1.14
NCS^-	385	5.79	483	7.05	583	0.87	619	0.99	12.84	98	1.22	1.14
Cl^-	375	4.88	477	9.85	583	0.81	619	0.96	14.7	102	2.02	1.18
Br^-	380	6.27	486	8.32	588	0.79	624	1.06	14.6	106	1.33	1.34
N_3^-	382	5.84	486	5.85	590	0.65	628	0.94	11.7	104	1.00	1.45
CN^-	387	5.28	495	5.51	600[b]	0.56[b]	640	0.90	10.8	108	1.04	1.61
I^-	388	7.18	498	4.66	598[b]	0.58[b]	634	0.98	11.84	110	0.65	1.69

[a] 10^{-4} molar extinction coefficient. [b] Unresolved shoulder. [c] Not determined because of poor solubility or instability. [d] In toluene.

It is a little perplexing that the strength of the B-CT CI as measured by $\Delta\lambda$(V–VI) is not mirrored in the $\epsilon(V)/\epsilon(VI)$ ratios. Suggestively however, the strength of the B-CT CI measured by $\Delta\lambda$(V–VI) increases with charge donation from the $a_1(\pi)$ orbital measured by $\epsilon(III)/\epsilon(IV)$. It would seem that $\Delta\lambda$(V–VI) is quite sensitive to an orbital contraction enhancement of the B-CT CI. A contraction of the $a_1(\pi)$ orbital might also increase the B-Q CI and so explain the shift to longer wavelengths of bands III and IV with rising $\epsilon(III)/\epsilon(IV)$. It would also be reasonable to expect this contraction effect to be offset to some extent by a reduction of B-Q CI through the loss of HOMO degeneracy. The band V and VI wavelength pattern suggests that the strength and polarizability of the electrostatic field surrounding the axial ligand has a direct influence on the B-CT excited-state energies.

Interestingly, the dissolution of $(TPP)Mn(H_2O)_2B(C_6H_5)_4$ in purified CH_2Cl_2 results in a rapid conversion to [(TPP)Mn(Cl)], within minutes at 10^{-5} M, and the decomposition is only slightly slower for $(TPP)Mn(DMF)_2B(C_6H_5)_4$. Axial ligation or counterion contact binding at the metal would appear to be essential for the prevention of solvent breakdown. The tetraphenylborate salts are more stable in toluene, where the optical spectrum is much like that of $(TPP)Mn(H_2O)_2ClO_4$ in the same solvent (Figure 3). Band V appears at 480 nm, suggesting that the B-CT CI is even weaker for $(TPP)Mn(H_2O)_2B(C_6H_5)_4$ than for $(TPP)Mn(H_2O)_2ClO_4$. Figure 3 indicates that the fading CT intensity is rekindled in an aromatic solvent, as a result of mixing of the metalloporphyrin and solvent π systems. The particular mechanism will require a theoretical elaboration.

Carbon-13 NMR and Spin Distributions. The Karplus–Fraenkel equation[103] provides a theoretical account of carbon-13 hyperfine coupling in molecules carrying spin in $p(\pi)$ orbitals. Of the complexes listed in Tables 1 and 2, the macrocycles of the acetato, nitrato, and perchlorato complexes seem least likely to be contaminated with σ spin (*vide supra*). Accordingly, the ^{13}C spectra of these complexes are most likely to be amenable to a Karplus–Fraenkel analysis. The effective ligand field strengths of the acetate, nitrate, and perchlorate axial ligands virtually span the range of field strengths exerted by the axial ligands of Table 1. Consequently, the results of a Karplus–Fraenkel analysis applied to the acetato, nitrato, and perchlorato complexes should provide a reasonable basis for the interpretation of the ^{13}C spectra of other (TPP)Mn(X) complexes.

The carbon-13 NMR spectra for a number of (TPP)Mn(X) complexes dissolved in CD_2Cl_2 at 25 °C are summarized in Table 3. The proton and carbon-13 NMR spectra of $(TPP)Mn(H_2O)_2ClO_4$ in CD_2Cl_2 are shown in Figures 4 and 5. Infrared, optical, and NMR spectroscopy to be discussed at a later date[97] indicates that at NMR concentrations (saturated at 2.2×10^{-2} M) the solution species is in equilibrium between [(TPP)Mn(ClO_4)] and [(TPP)Mn(H_2O)(ClO_4)], and we believe that the latter is predominant under the NMR experimental conditions. However for convenience the solution species will be referred to as [(TPP)Mn(ClO_4)]. Perchlorato manganese complexes are known[96] to decompose to chloro complexes in chlorinated solvents. Accordingly highly purified solvents were used throughout this work and solutions were spectroscopically monitored for any decomposition. This was of particular concern in the typically 12-h carbon-13 NMR experiments; however, there was no difference in the proton spectrum recorded before and after the carbon-13

Table 3. Carbon-13 NMR Features for (TPP)Mn(X) in CD_2Cl_2[a]

	pyrrole			phenyl				conc
X⁻	α	β	*meso*	quart.	*ortho*	*meta*	*para*	(10^{-2} M)
NCO^-	396	−156	126	199	169.8	131.3	131.1	5.96
$CH_3CO_2^-$	413	−165	117	206	162.2	130.9	130.5	6.47
Cl^-	393	−158	110	204	167.9 166.2	131.6	131.0	6.32
Br^-	398	−163	95	210	166.6 163.7	131.6	131.0	5.59
I^-	408	−158	65	217	160.6	131.6	131.0	3.36
NCS^-	398	−166	100	209	161.2	130.7	130.7	5.59
NO_2^-	430	−179	88	218	151.5	130.1	130.1	3.27
NO_3^-	418	−192	68	226	143.8	129.5	129.5	4.48
CN^-	408	−144	91	204	176 165	132.7	132.1	6.48
ClO_4^-	419	−204	23	245	125.2	128.3	128.8	2.20
Zn(TPP)	150.8	132.5	143.3	121.6	134.9	127.5	128.0	

[a] At 25 °C and referenced against TMS in ppm.

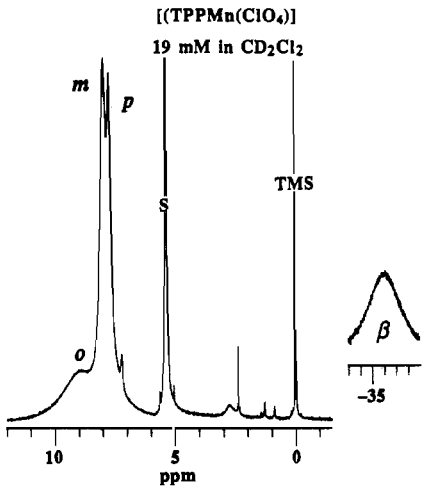

Figure 4. Proton NMR spectrum of $(TPP)Mn(H_2O)_2ClO_4$ in CD_2Cl_2 at 19 mM and 25 °C. The solvent is indicated with an S, and TMS is used as an internal reference.

(103) Karplus, M.; Fraenkel, G. K. *J. Chem. Phys.* **1961**, *35*, 1312.

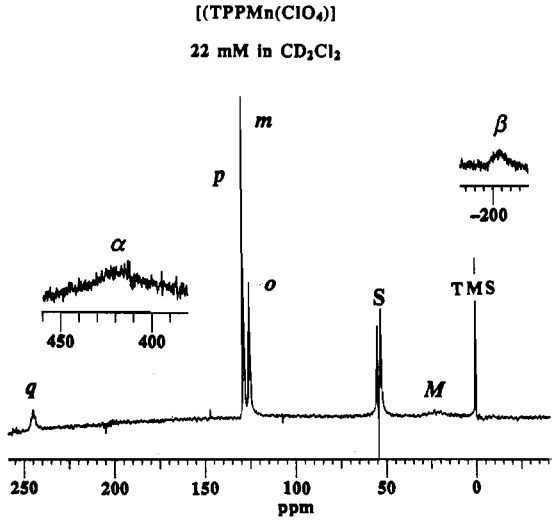

Figure 5. Carbon-13 spectrum of (TPP)Mn$(H_2O)_2ClO_4$ in CD_2Cl_2 at 22 mM and 25 °C. The symbols indicate the phenyl quaternary carbon *q*, the α-carbon α, phenyl *para*, *meta*, and *ortho*-carbon atoms *o*, *m*, and *p*, the *meso* quaternary carbon *M*, and the β-carbon β. The solvent is indicated with S, and TMS is used as an internal reference. The intense solvent peak has folded back.

NMR measurements. The [(TPP)Mn(ClO_4)] ^{1}H and ^{13}C spectra are both quite unlike the other [(TPP)Mn(X)] spectra (Tables 1 and 3).

There are in general three contributions to an NMR isotropic shift:

$$\Delta H^{iso}/H = \Delta H^{M}/H + \Delta H^{L}/H + \Delta H^{con}/H \quad (1)$$

The first term on the right-hand side of eq 1 represents a metal-centered dipolar shift, the second term is a ligand-centered pseudocontact shift, and the third term is the Fermi contact or scalar isotropic resonance shift. In formally manganese(III) complexes having a tetragonal distortion, the C_{2v} $^5A_1$ electronic ground state is well separated from the first excited state, by several thousand wavenumbers,[104] and minimal spin–orbit coupling ensures g-tensor isotropy.[105] It follows then[105-108] that for a carbon-13 or proton nucleus (indicated by I)

$$\frac{\Delta H^{con}}{H} = -A^{I}\frac{|\gamma_e|S(S+1)}{|\gamma_I|\,3kT} \quad (2)$$

and for aromatic protons the hyperfine coupling constant is given by the McConnell equation[109,110]

$$A^{H} = Q^{H}_{CH}\rho^{C}(\pi)/2S \quad (3)$$

in which –63 MHz is used for Q^{H}_{CH}. The carbon-13 hyperfine coupling constant is given by the Karplus–Fraenkel equation

$$A^{C} = (S^{C} + \sum_{i=1}^{3} Q^{C}_{CX(i)})\rho^{C}(\pi) + \sum_{i=1}^{3} Q^{C}_{X(i)C}\rho^{X(i)}(\pi) \quad (4)$$

in which the constants have been calculated and verified experimentally:[111] S^{C} = –35.5 MHz, Q^{C}_{CH} = 54.6 MHz, $Q^{C}_{CC'}$ = 40.3 MHz, $Q^{C}_{C'C}$ = –39 MHz. It is assumed[112] that $Q^{C}_{CN} = Q^{C}_{CC'}$ and $Q^{C}_{NC} = Q^{C}_{C'C}$. The Karplus–Fraenkel equation describes the hyperfine coupling constant for the special case $S = {}^1/_2$; for the more general case of $S > {}^1/_2$, the coupling constant must be divided by the spin normalization factor $2S$.[31,113,114]

Given g-tensor isotropy, the metal-centered dipolar contribution is given[115] by

$$\Delta H^{M}/H = A_m G \quad (5)$$

where *G* is a simple geometric factor[111,116-118] that is negative for the porphyrin nuclei. The A_m term describes the magnetic anisotropy

$$A_m = \frac{\mu_o\beta^2(\mu_\perp{}^2 - \mu_\parallel{}^2)}{4\pi 9kT} \quad (6)$$

Behere and Mitra[105] have derived a relationship between the zero field splitting parameter *D* and the effective magnetic moment components $\mu_\perp$ and $\mu_\parallel$

$$\mu_\parallel = \frac{6g_\parallel{}^2(e^{-D/kT} + 4e^{-4D/kT})}{(1 + 2e^{-D/kT} + 2e^{-4D/kT})} \quad (7)$$

$$\mu_\perp = \frac{g_\perp{}^2 kT}{D}\frac{(18 - 14e^{-D/kT} - 4e^{-4D/kT})}{(1 + 2e^{-D/kT} + 2e^{-4D/kT})} \quad (8)$$

and in formally manganese(III) porphyrin complexes $g_\perp = g_\parallel = 2$. Additionally, Mispelter et al.[119] have stated that the ligand-centered pseudocontact shift is proportional to the magnetic anisotropy in complexes having an orbitally nondegenerate ground state and accordingly

$$\frac{\Delta H^{L}}{H} = -\frac{\beta^2(\mu_\perp{}^2 - \mu_\parallel{}^2)}{18kT}\frac{2b/\hbar}{\gamma_e\beta}\rho^{C}(\pi) \quad (9)$$

The ligand-centered pseudocontact shift[107] arises from the mixing of anisotropic metal orbitals with compatible ligand orbitals. Only those nuclei having the lobes of such orbitals centered upon them are subjected to ligand-centered pseudocontact shifts.

Equations 2–9 were applied to the proton and carbon-13 spectra of the [(TPP)Mn(CH_3CO_2)], [(TPP)Mn(NO_3)], and [(TPP)-Mn(ClO_4)] complexes, and the results of this application are summarized in Tables 4–8. The calculation of pseudocontact shift contributions requires a knowledge of the zero field splitting parameter *D*; however, *D* values have not yet been determined

Table 4. Magnetic Anisotropy Data for Selected [(TPP)Mn(X)]

	D (cm^{-1})[a]	$\Delta\mu^2$ (μ_B)	$\mu_\perp$ (μ_B)	$\mu_\parallel$ (μ_B)
$CH_3CO_2^-$	–2	–0.4889	4.8823	4.9321
NO_3^-	–1	–0.2439	4.8907	4.9155
ClO_4^-	1	0.2431	4.9072	4.8824

[a] *D* value assignment is described in main text.

(104) Behere, D. V.; Marathe, V. R.; Mitra, S. *Chem. Phys. Lett.* **1981**, *81*, 57.
(105) Behere, D. V.; Mitra, S. *Inorg. Chem.* **1980**, *19*, 992.
(106) Wüthrich, K.; Baumann, R. *Helv. Chim. Acta.* **1973**, *56*, 585.
(107) Kurland, R. J.; McGarvey, B. R. *J. Magn. Reson.* **1970**, *2*, 286.
(108) Bloembergen, N. *J. Chem. Phys.* **1957**, *27*, 595.
(109) McConnell, H. M. *J. Chem. Phys.* **1956**, *24*, 764.
(110) McConnell, H. M.; Chestnut, D. B. *J. Chem. Phys.* **1958**, *28*, 107.
(111) Goff, H. M. *J. Am. Chem. Soc.* **1981**, *103*, 3714.
(112) Neely, J. W.; Lam, C. H.; Kreilick, R. E. *Mol. Phys.* **1975**, *29*, 1663.
(113) Drago, R. S. *Physical Methods for Chemists*, 2nd ed.; Saunders College Publishing: New York, 1992.
(114) La Mar, G. N. *Inorg. Chem.* **1971**, *11*, 2633.
(115) Horrocks, W. D., Jr. *NMR of Paramagnetic Molecules*; Academic Press: New York, 1973.
(116) La Mar, G. N.; Walker, F. A. *J. Am. Chem. Soc.* **1973**, *95*, 1782.
(117) La Mar, G. N. *NMR of Paramagnetic Molecules*; Academic Press: New York, 1973.
(118) Goff, H. M.; La Mar, G. N.; Reed, C. A. *J. Am. Chem. Soc.* **1977**, *99*, 3641.
(119) Mispelter, J.; Momenteau, M.; Lhoste, J.-M. *J. Chem. Soc., Dalton Trans.* **1981**, 1729.

Table 5. Carbon-13 Dipolar Shifts for Selected [(TPP)Mn(X)]

	D (cm^{-1})[a]	$\Delta H^M(\beta)/H$	$\Delta H^L(\beta)/H$	$\Delta H^M(\alpha)/H$	$\Delta H^L(\alpha)/H$	$\Delta H^M(M)/H$	$\Delta H^L(M)/H$
$CH_3CO_2^-$	−2	1.5	11.0	4.1	0	2.8	56
NO_3^-	−1	0.7	6.7	2.0	0	1.4	30
ClO_4^-	1	−0.4	−8.2	−2.0	0	−1.4	−30

[a] D value assignment is described in main text; shifts are in ppm.

Table 6. Proton Contact Shifts for Selected [(TPP)Mn(X)]

	D (cm^{-1})[a]	β	*ortho*	*meta*	*para*
$CH_3CO_2^-$	−2	29.8	*b*	−0.68	0.27
NO_3^-	−1	36.55	*b*	−0.52	0.22
ClO_4^-	1	45.05	−0.55	−0.05	0.13

[a] D value assignment is described in main text; shifts are in ppm. [b] Not observed.

Table 7. Calculated Spin Densities at Porphyrin Core Sites of Selected [(TPP)Mn(X)][a]

	β	α	*meso*	nitrogen
$CH_3CO_2^-$	0.009	0.049	0.046	0.019
NO_3^-	0.011	0.056	0.048	0.031
ClO_4^-	0.014	0.063	0.049	0.044

[a] Spin densities are normalized.

Table 8. Contribution of Porphyrin Nuclei Spin Densities to Carbon-13 Contact Shifts (ppm) of [(TPP)Mn(ClO_4)]

site	α	β	*meso*	nitrogen	total
α	−1132	111	399	361	−261
β	517	−283 + 111[a]	0	0	345
meso	1034[b]	0	−863	0	161

[a] Contribution from neighboring β-carbon spin density. [b] Sum of contributions from both adjacent α-carbon densities.

for these complexes. Dugad et al.[120] have reported a second-order perturbation treatment of the relationship between the zero-field splitting and tetragonal distortions in the ligand field of manganese porphyrin complexes. This model was used as a guide in assigning values of D to [(TPP)Mn(CH_3CO_2)], [(TPP)Mn(NO_3)], and [(TPP)Mn(ClO_4)]. Solid-state measurements[41,104,105] suggest that for manganese porphyrins -3 cm$^{-1} < D < 3$ cm^{-1}. The small zero-field splittings in manganese porphyrins produce pseudocontact shifts that are small[29,92] and so are not a critical complication in the calculation of spin densities. The ligand field model of Dugad et al. indicates that the stronger the axial ligand field and the smaller the tetragonal distortion, then the more negative the zero field splitting parameter. In the spirit of the Dugad model, zero-field splittings of -2, -1, and $+1$ cm^{-1} are assigned to the $CH_3CO_2^-$, NO_3^-, and ClO_4^- complexes, respectively. The optical and NMR spectroscopies confirm that the ligand field strength declines in the order $CH_3CO_2^- > NO_3^- > ClO_4^-$ (*vide infra*). Additionally, the downfield appearance of the phenyl *ortho* proton signal of [(TPP)Mn(ClO_4)] provides circumstantial evidence of a small positive zero field splitting parameter in this complex (no σ spin evident). The *ortho* proton can also be detected in the NMR spectrum of [(TPP)Mn(I)], and La Mar and Walker[92] have proposed a positive zero field splitting parameter for this complex on the basis of a comparative line width analysis of the methyl proton resonance signal of ($TP_{4\text{-}CH_3}P$)Mn(X) (X = F, N_3, Cl, Br, I). The phenyl para proton line widths of the complexes used in this study have not been used for the assignment of D values, because the *para* protons are not isolated from spin effects and so cannot give a reliable measure of dipolar relaxation.

Although Dugad et al.[120] have concluded that the sign and magnitude of the zero field splitting parameter depends on the nature of the ligand field tetragonal distortion in manganese porphyrin complexes, it is suggestive that the apparent shift[92] in negative to positive values follows an increase in spin transferred to the equatorial ligand (a positive D value means that $m_\perp > m_\parallel$). Perhaps the spin–orbit coupling from excited states is so weak that the geometry of the spin distribution makes a significant contribution to zero-field splitting.

Equation 3 was used to obtain a spin density at the β-pyrrole carbon site from the proton contact shift. The carbon contact shifts were then employed in eq 4 to calculate spin densities at the α-pyrrole and *meso* carbon sites and the pyrrole nitrogen site. Although the $a_2(\pi)$ porphyrin HOMO has the same symmetry as the metal d_{xy} orbital, any orbital interaction is severely restricted by minimal overlap. Accordingly, it was assumed that there is no ligand-centered pseudocontact shift at the α-pyrrole carbon. A further assumption was made in calculating the spin density at the *meso* carbon site. La Mar and Walker[116] established that steric constraints attenuate phenyl contact shifts by at least a factor of 10. That is, any *meso* $b_1(\pi^*)$, $b_2(\pi^*)$ orbital $p(\pi)$ spin can only be weakly delocalized into the phenyl appendages. The HOMO and LUMO of a phenyl residue both have nodes at the *meta* positions and consequently any delocalized $p(\pi)$ spin will concentrate at the phenyl *ortho* and *para* carbon atoms. It seems reasonable to assume then, that the $p(\pi)$ density at the phenyl quaternary carbon site is effectively zero (such spin density is to be distinguished from polarization-correlation effects) and that polarization-correlation effects from *ortho* $p(\pi)$ spin are too weak to travel into the *meso* position. Additionally, having no apriori knowledge of the *meso* spin density and hence *meso*-centered ligand pseudocontact shift, an initial spin density was calculated by assuming no ligand-centered pseudocontact shift. A ligand pseudocontact shift was then determined with that spin density and incorporated in a recalculation of the *meso* spin density. The refinement process was repeated until the calculated ligand pseudocontact shifts differed by no more than 1 ppm (2 cycles for ClO_4^- and NO_3^- and 3 cycles for $CH_3CO_2^-$).

The Karplus–Fraenkel analysis of contact shifts precludes a determination of the influence of the α-pyrrole carbon $p(\pi)$ spin density on the β-pyrrole proton contact shift. A future line width analysis may provide the required independent assessment of the β-pyrrole $p(\pi)$ spin density. The obviously high α-pyrrole carbon $p(\pi)$ spin density is likely to impose a downfield bias on the β-pyrrole proton contact shift, which means that the calculated spin densities are then under estimates.

The α-pyrrole carbon $p(\pi)$ spin density is so large that it effectively determines the carbon-13 spectroscopy (Tables 7 and 8). Polarization and correlation from this large spin density explains the alternation of shift signs for the α- and β-pyrrole carbon signals noted by Goff and Hansen.[30] The α-pyrrole carbon $p(\pi)$ spin density overcomes the covalent spin in the small β-pyrrole carbon $b_1(\pi)$ and $b_2(\pi)$ orbital lobes, such that a net negative spin density at the β-pyrrole carbon nucleus results in the observed upfield resonance shift. Domination of the spin density at the *meso* carbon nucleus by the α-pyrrole carbon $p(\pi)$ spin density explains the optical-NMR spectroscopy paradox noted by La Mar and Walker.[29] Although the optical spectroscopy of manganese porphyrins is a manifestation of heavy mixing of the porphyrin LUMO and metal d_{xz} and d_{yz} orbitals,[48,53] proton NMR spectroscopy suggested little $p(\pi)$ density at the *meso* position (where the porphyrin LUMO has large lobes). However the spin density is in fact high at the *meso* position, as indeed indicated by the optical spectroscopy, but it is undermined by polarization

(120) Dugad, B.; Behere, D. V.; Marathe, V. R.; Mitra, S. *Chem. Phys. Lett.* **1984**, *104*, 353.

and correlation from the two neighboring α-pyrrole carbon p(π) spin densities. Spin polarization from the α-pyrrole carbon p(π) spin density also determines the phenyl quaternary carbon-13 resonance.

Although the *meso* and quaternary carbon-13 resonances are dominated by polarization from the α-pyrrole carbon spin, they are also modulated by the presence of the considerable positive π spin density at the *meso* position, generated in the porphyrin $b_1(\pi^*)$, $b_2(\pi^*)$ orbitals through a dispersal of spin from the symmetry-compatible metal $b_1(3d_{xz})$ and $b_2(3d_{yz})$ orbitals. It is a little surprising that the *meso* positive p(π) density is greatest for [(TPP)Mn(ClO_4)]. The π spin delocalization into the phenyl residues increases with increasing ligand field strength, in an apparent contradiction to the decline in positive spin at the *meso* position. It would seem that a stronger axial ligand field promotes spin transfer to the phenyl residue LUMO, at the expense of the *meso* density.

The phenyl nuclei are also affected by residual polarization from the α-pyrrole carbon spin. The observed contact shifts apparently reflect an axial ligand dependent balance of this polarization, with the delocalized positive porphyrin $b_1(\pi^*)$, $b_2(\pi^*)$ orbital spin. The *ortho* proton contact shift of [(TPP)Mn(ClO_4)], given in Table 7, suggests that the faded α-pyrrole spin polarization is actually dominant at this position (in this complex), whereas the para proton resonance suggests dominance of the delocalized positive p(π) spin at this position. Any interpretation of the phenyl proton resonances is most particularly contingent on the value of the zero field splitting parameter (because of the low level of spin delocalization).

Surprisingly, the carbon-13 NMR spectra of [(TPP)MnCl)], [(TPP)Mn(Br)], and particularly [(TPP)Mn(CN)] exhibit split phenyl *ortho* signals of the kind found in the *ortho* and *meta* carbon-13 resonances of high-spin iron(III) porphyrin spectra.[28,119] In the iron complexes, the splitting is the result of doming of the porphyrin core, a large metal ion displacement, and a larger zero-field splitting (e.g. 10 cm^{-1}) than found in manganese porphyrins. The two *ortho* carbons in a phenyl moiety thus undergo different pseudocontact shifts. The metal ion displacement and zero-field splitting is considerably smaller in manganese porphyrins, and the porphyrin core has a quasi S_4 ruffle in which the pyrrole units either alternately tilt up and down or in a side to side fashion.

The three complexes that have split *ortho* carbon peaks also have among the highest ϵ(III)/ϵ(VI) band ratios (Table 2), which provide an indicator of $a_1(\pi)$ to d_{z^2} σ bonding. The other complexes which show signs of σ bonding have heavily broadened *ortho* signals that appear close to resolution. Conversely, the complexes that have hard oxy ligands and minimal σ bonding, display comparatively sharp *ortho* signals (Figure 6). HOMO level σ bonding would be favored by a core ruffle in which the pyrrole groups alternately tilt up and down rather than side to side (i.e. a *sad* rather than *ruf* core conformation). It seems reasonable to conclude that in solution σ bonding encourages *sad* core ruffling and that this results in differences in the phenyl carbon isotropic shifts, particularly for the *ortho* carbon resonances. Whether this is caused by asymmetry in the pseudocontact or contact interaction (and therefore orbital mixing) or both remains to be established. It may be relevant that the cyano complex displays the largest *ortho* carbon signal splitting and also has an unusual optical spectrum. The very unusual nature of the optical spectrum of the cyano complex is most evident in toluene,[121] in which bands III–V spearate into distinct pairs.

As Figures 6 and 7 indicate, the line width of the *ortho* signal is solvent and temperature sensitive and, hence, viscosity sensitive. In $CDCl_3$ at 25 °C the cyano *ortho* phenyl carbon signals have approximately the same width and height as the quaternary resonance of Figure 7, but on warming to 45 °C they widen to become similar to the *ortho* peaks observed in CD_2Cl_2 at 25 °C (Figure 6). The *meta* peak also exhibits some sensitivity and is halved in height on changing from CD_2Cl_2 to $CDCl_3$. The *ortho*

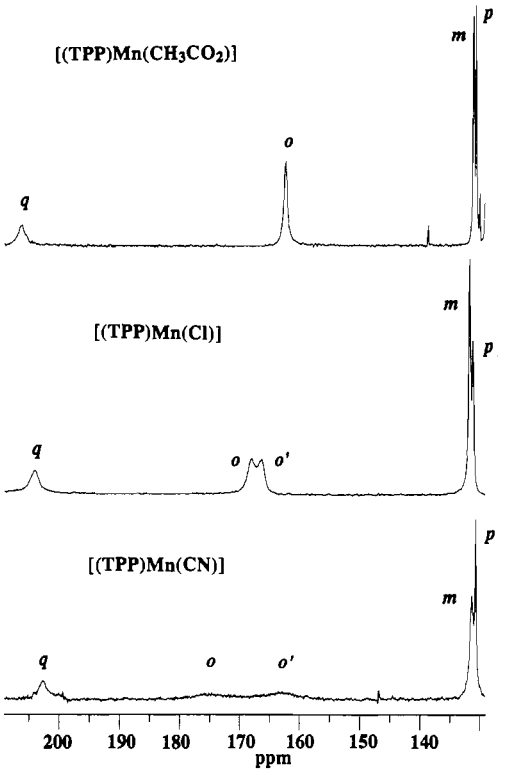

Figure 6. Phenyl *q*, *o*, *m*, and *p* carbon region in the carbon-13 spectra of [(TPP)Mn(CH_3CO_2)], [(TPP)Mn(Cl)], and [(TPP)Mn(CN)] in CD_2Cl_2 at 25 °C. Toluene solvate signals are present in the [(TPP)Mn(CH_3CO_2)] spectrum. The *o*, *m*, *p*, and *q* symbols indicate the phenyl *ortho*, *meta*, *para*, and quaternary carbon resonances.

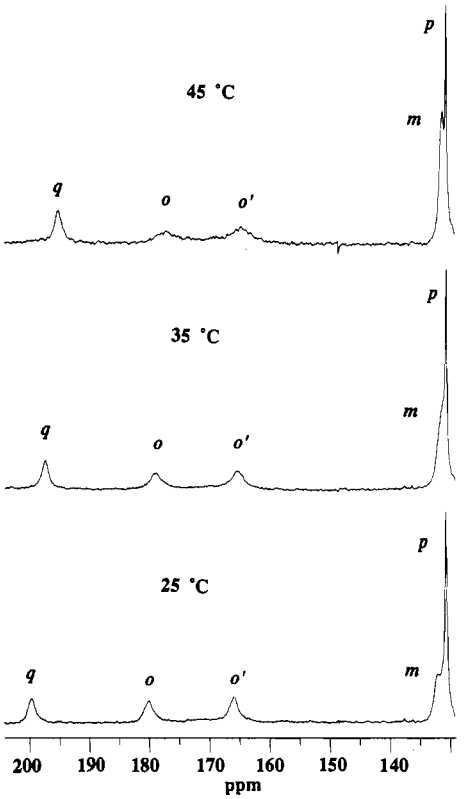

Figure 7. Temperature-dependent changes in the *ortho* carbon signals of [(TPP)Mn(CN)] dissolved in $CDCl_3$. The *o*, *m*, *p*, and *q* symbols indicate the phenyl *ortho*, *meta*, *para*, and quaternary carbon resonances, respectively.

(121) Wayland, B. B.; Olson, L. W.; Siddiqui, Z. U. *J. Am. Chem. Soc.* **1976**, *98*, 94.

peaks of [(TPP)Mn(Cl)] are not resolved in $CDCl_3$ at 25 °C; however, they are resolved on warming to 45 °C. The solvent viscosity apparently influences the complex conformation extension in solution. The increased broadening at lower viscosity may indicate a second signal separation or an increase in relaxation rate brought on by an increase in spin density.

Valence State. There would seem to be two possible explanations for the high-spin level at the α-pyrrole carbon location. The first explanation is that mixing of the meta d_{xz} and d_{yz} orbitals with the porphyrin LUMOs increases the size of the small α-pyrrole carbon LUMO lobe so much that it becomes larger than the *meso* lobe. This seems physically implausible. The calculated spin densities at the *meso* carbon and pyrrole nitrogen sites are consistent with a minimal perturbation of the free ligand LUMO topology. Were the α-pyrrole carbon LUMO lobe to be larger than the *meso* lobe, then the pyrrole nitrogen lobe would be larger still and positive spin at this site would induce an upfield α-pyrrole carbon resonance.

A second explanation is that the manganese porphyrin complexes have a significant $(d_{x^2-y^2})^0 (d_{z^2})^1 (d_{xz}\, d_{yz})^2 (d_{xy})^2 (a_2(\pi))^1 (a_1(\pi))^2$ $[Mn^{II}P^{\bullet-}]^+$ valence-state contribution to the electronic ground state. The α-pyrrole carbon p(π) spin densities in Table 7 are very similar to those recently determined[122] for two iron(II) nitrosyl chlorin π cation radicals and in accord with theoretical[59,64,123,124] porphyrin π cation radical spin densities. That the high-spin formulation originally proposed by Richert et al.[26] should be discarded in favor of an intermediate spin formulation is required by the NMR spectroscopy. The occupation of the $d_{x^2-y^2}$ is known to result in characteristically large downfield contact shifts, as a result of heavy σ spin transfer into the porphyrin ligand.[28,119] A $(d_{x^2-y^2})^0 (d_{z^2})^1 (d_{xy})^1 (d_{xz}\, d_{yz})^3 (a_2(\pi))^1 (a_1(\pi))^2$ $[Mn^{II}P^{\bullet-}]^+$ state may also be discounted, as antiferromagnetic coupling between the a_2 orbitals would produce a detectably lower effective magnetic moment than found experimentally.[22,41,105]

The spin density at the α-carbon is clearly dependent on the axial ligand, and it would thus appear that the $(d_{x^2-y^2})^0 (d_{z^2})^1 (d_{xz}\, d_{yz})^2 (d_{xy})^2 (a_2(\pi))^1 (a_1(\pi))^2$ $[Mn^{II\bullet-}]^+$ valence state need not be pure. There are then three possibilities: (1) There is some weak mixing between the metal $(a_2(3d_{xy}))^2$ orbital and the porphyrin $(a_2(\pi))^1$ orbital that depends on the ligand field strength of the axial ligand. (2) There is an axial ligand dependent valence-state isomerization[118] equilibrium between $(a_2(3d_{xy}))^2 (a_2(\pi))^1$ and $(a_2(3d_{xy}))^1 (a_2(\pi))^2$. (3) The electronic ground state is an axial ligand dependent quantum mechanical admixture[119,120] of the $[Mn^{II}P^{\bullet-}]^+$ and $[Mn^{III}P^{2-}]^+$ valence states. The mechanism of the axial ligand dependence has yet to be determined, although the first possibility seems least likely. That the ground state need not be pure perhaps provides an explanation for the Goff and Hansen[30] observation of a lack of Curie law temperature dependence of the α-pyrrole carbon-13 resonance in manganese porphyrin complexes. The deuterium NMR spectra of the two iron(II) nitrosyl chlorin π cation radicals, mentioned above, also exhibit non-Curie law behavior, and this is attributed to a thermal admixture of two valence states.[122]

At this stage it should be mentioned that in 1980 Mishra, Chang, and Das[56,61] reported extended Hükel calculations of the hyperfine interaction in pentacoordinate Mn(III) porphyrin complexes. These calculations were restricted to the $[Mn^{III}P^{2-}]^+$ state, and very different spin distributions were found.

The optical spectrum of $[(TPP)Mn(ClO_4)]$ is almost identical to the methylene chloride spectrum of the manganese(III) porphyrin π cation radical described by Goff et al.,[34] $[(TPP)Mn(Cl)]ClO_4$ (Figure 3; *viz.* a Soret band at 487 nm, ε(V)/ε(VI) ratio of 0.59, ε(V) + ε(VI) = 9.3×10^4). The spectrum is also similar to that of the $(TPP)Mn^{III}(Cl)SbCl_6 \cdot 4C_2H_2Cl_4$ complex structurally characterized by Spreer et al.[35] and first described by Carnieri et al.[36] The optical spectra of $[(TPP)Mn(ClO_4)]$, $[(TPP)Mn^{III}(Cl)]SbCl_6$, and $[(TPP)Mn^{III}(Cl)]ClO_4$ being essentially the same demonstrates that the electron populations in the B and CT states are the same and that the chloro ligand compensates for the lower lying Mn(III) valence levels of the latter $[Mn^{III}P^{\bullet-}]^{2+}$ complexes. Slight differences in the spectra of $[(TPP)Mn^{III}(Cl)]ClO_4$ and $[(TPP)Mn^{III}(Cl)SbCl_6$ indicate that the very weak counterions also coordinate in solution.

Oxidation of the porphyrin ligand need not undermine its capacity to function as a donor ligand. The −36 ppm β-pyrrole proton resonance in the NMR spectrum of $[(TPP)Mn(ClO_4)]$ is in fact less than the −39 ppm of the $[(TPP)Mn^{III}(Cl)]ClO_4$ complex.[34] This may reflect the reduced effective metal charge and the slightly higher energy of the Mn(II) valence orbitals.[53,55,78] The double-ζ basis set modeling of iron porphyrin reported by Kashiwagi and Obara[60] shows that electron loss from the porphyrin ligand has a comparatively minor impact on the macrocycle electronic topology. The INDO/S-CI modeling of Edwards and Zerner[124] indicates that the HOMO energy is not significantly altered by electron loss.

It is noteworthy that although the $[(TPP)Mn(ClO_4)]$ complex has a high spin density in the $a_2(\pi)$ porphyrin orbital, the X-band EPR spectrum of $[(TPP)Mn(ClO_4)]$ in methylene chloride is silent down to 77 K. In contrast $[(TPP)Mn^{III}(Cl)]ClO_4$ has a broad $g = 2$ feature at 77 K that is attributed to the $^2A_2$ macrocycle radical,[34] yet $[(TPP)Mn^{III}(Cl)]SbCl_6$ is silent[35] down to 8 K. The latter complex additionally fails to show the 1290-cm^{-1} IR band that has been used as a marker for porphyrin ligand oxidation.[125,126] There is no indication of such a band in the solution- or solid-state IR spectra of $[(TPP)Mn(ClO_4)]$. The two iron(II) nitrosyl chlorin π cation radicals mentioned earlier are also EPR silent down to 77 K.[122]

The solid-state magnetic measurements of Brackett, Richards, and Caughey,[25] Kennedy and Murray,[41] and Behere, Marathe, Dugad, and Mitra[104,105,120] leave no doubt that (TPP)Mn(X) complexes behave magnetically as $S = 2$ spin systems. The carbon-13 spectroscopy suggests a mixed $[Mn^{II}(S = {}^3/_2, {}^4A_2)P\text{-}(S = {}^1/_2, {}^2A_2)^{\bullet-}]^+ + [Mn^{III}(S = 2, {}^5A_1)P^{2-}]^+$ valence state. These two different physical views of the same complexes are not in conflict. The symmetry of the spin orbitals is the same for both electronic configurations; both valence-state components have an $S = 2$ $^5A_1$ ground state spin manifold.

Comparatively strong axial ligand fields are apparently required to support the $[Mn^{III}(S = 2, {}^5A_1)P^{2-}]^+$ state. A logical extension of this requirement is found in Wayland, Olson, and Siddiqui's demonstration[121] that in (TPP)Mn(X)(NO) complexes, the axial ligand system is oxidized. More recently, bis(cyano) and bis(hydroxo) coordination to manganese porphyrins has also been found to result in oxidation of the axial ligand.[33,127] Simply dissolving $(TPP)Mn(H_2O)_2ClO_4$ in triethylamine immediately produces the characteristic optical signature of a manganese(II) porphyrin. In this context it is also worth recalling the slow ligand autoxidation suffered by $[(EDTA)Mn(H_2O)]^-$.

Richert, Tsang, and Sawyer's proposition[26] of a $[Mn^{II}(S = {}^5/_2)P^{\bullet-}]^+$ valence state for manganese porphyrins was based on electrochemical and X-ray absorption measurements that could be accommodated by porphyrin to metal covalency in a formal $[Mn^{III}P^{2-}]^+$ valence state. Given that the proposal included back-bonding from the metal to the oxidized porphyrin orbital, the proposition is in essence a semantic variation of the $[Mn^{III}P^{2-}]$ valence-state description. This is not so for the $[Mn^{II}(S = {}^3/_2,$

(122) Ozawa, S.; Fujii, H.; Morishima, I. *J. Am. Chem. Soc.* **1992**, *114*, 1548.
(123) Fajer, J.; Borg, D. C.; Forman, A.; Dolphin, D.; Felton, R. H. *J. Am. Chem. Soc.* **1970**, *92*, 3451.
(124) Edwards, W. D.; Zerner, M. C. *Can. J. Chem.* **1985**, *63*, 1763.
(125) Jones, D. H.; Hinman, A. S. *J. Chem. Soc., Dalton Trans.* **1992**, 1503.
(126) Shimomura, E. T.; Phillippi, M. A.; Goff, H. M. *J. Am. Chem. Soc.* **1981**, *103*, 6778.
(127) Hansen, A. P.; Goff, H. M. *Inorg. Chem.* **1984**, *23*, 4519.

$^4A_2)P(S = {}^1/_2, {}^2A_2)^{\bullet-}]^+$ state, because the critical porphyrin $a_2(\pi)$ HOMO and metal $3d_{xy}$ orbitals cannot significantly overlap.

The $^6A_1$ d^5 Mn(II) ion is known to be significantly pushed out of a domed P^{2-} porphyrin core,[78] as the result of the electrostatic repulsion associated with an occupied metal $d_{x^2-y^2}$ orbital. It is perhaps because of this consequence of $d_{x^2-y^2}$ orbital occupation, that the $^6A_1$ d^5 Mn(II) ion is not observed in the NMR spectroscopy of [(TPP)Mn(X)] complexes. The crystal structures of (TPP)Mn(X) complexes[43] show that the stronger the axial ligand field, then the larger the metal ion displacement from the porphyrin core. The poor metal ion charge compensation associated with a weak axial ligand field encourages a greater degree of porphyrin to metal covalency. The result is a smaller displacement from the porphyrin core and an increase in the effective porphyrin ligand field strength. The $[Mn^{II}(S = {}^3/_2, {}^4A_2)P(S = {}^1/_2, {}^2A_2)^{\bullet-}]^+$ valence state may thus be a consequence of poor metal ion charge compensation from the axial ligand.

There is a parallel between manganese and iron porphyrins,[128-130] in that the $S = {}^3/_2$ state appears to be a consequence of weak axial ligation in both types of complex. Gregson[131,132] has determined a ligand field dependent spin-state phase diagram for the Mn(II) ion. Interestingly, the $Mn^{II}(S = {}^3/_2, {}^4A_2)$ ion is found in Mn(II) phthalocyanine,[133] whereas a spin equilibrium between $Mn^{II}(S = {}^3/_2, {}^4A_2)$ and $Mn^{II}(S = {}^5/_2, {}^6A_1)$ is observed in the weaker ligand field tetrasulfonated phthalocyanine complex.[134]

Conclusion. Axial ligand bonding in manganese tetraphenylporphyrin complexes may be significantly ionic in character and perhaps charge rather than orbital controlled. The crystal field component of the axial ligand field appears to be an important determinant of manganese porphyrin spectroscopy. Carbon-13 spectroscopy reveals that the chemically important valence state of manganese tetraphenylporphyrins is best formally described as an axial ligand dependent mixture of the C_{2v} $^5A_1$ $[Mn^{II}(S = {}^3/_2, {}^4A_2)P(S = {}^1/_2, {}^2A_2)^{\bullet-}]^+$ and $^5A_1$ $[Mn^{III}(S = 2, {}^5A_1)P^{2-}]^+$ spin manifolds. The compartmentalization of charge implicit in a formal valence state is generally rendered meaningless by covalency; however, in this particular case, it provides a simple summary of a valence state that has two components that are not related by covalency. Given that the calculated α-pyrrole spin densities are almost certainly underestimates, the $^5A_1$ $(d_{x^2-y^2})^0(d_{z^2})^1(d_{xz}d_{yz})^2(d_{xy})^2(a_2(\pi))^1(a_1(\pi))^2$ $[Mn^{II}P^{\bullet-}]^+$ state is probably the dominant partner, but the extent of this dominance is unclear. When the axial ligand field is very weak, the domination may be complete. The porphyrin $a_2(\pi)$ and metal $a_2(3d_{xy})$ orbitals are essentially covalently isolated, and therefore the description of the valence state is not just a question of semantics. A strong axial ligand field may lend support to the $[Mn^{III}(S = 2, {}^5A_1)P^{2-}]^+$ ground-state contribution, but the literature demonstrates that there is a point at which the axial ligand becomes formally oxidized and a $[Mn^{II}P^{2-}]$ derivative is formed.

Given that the porphyrin ligand field is tunable by peripheral substitution, it remains to be seen whether the $[Mn^{II}(S = {}^3/_2, {}^4A_2)P(S = {}^1/_2, {}^2A_2)^{\bullet-}]^+$ state establishes a presence in other manganese porphyrin complexes. Additionally, it is not yet known how the manganese porphyrin valence state is affected by interaction with the π system of aromatic solvents. Finally, the experimental chemistry of manganese porphyrin complexes sorely needs theoretical support, perhaps of the kind given to manganese phthalocyanines.[135]

Acknowledgment. This study was supported by the Australian Research Council.

(128) Goff, H.; Shimomura, E. *J. Am. Chem. Soc.* **1980**, *102*, 31.
(129) Boersma, A. D.; Goff, H. M. *Inorg. Chem.* **1982**, *21*, 581.
(130) Boersma, A. D.; Goff, H. M. *Inorg. Chem.* **1984**, *23*, 1671.
(131) Gregson, A. K. Ph.D. Thesis, University of Melbourne, 1974.
(132) Barraclough, C. G.; Gregson, A. K.; Mitra, S. *J. Chem. Phys.* **1974**, *60*, 962.
(133) Mitra, S. In *Progress in Inorganic Chemistry*; Lippard, S. J., Ed.; John Wiley: New York, 1977; Vol. 22; p 309.
(134) Moxon, N. T. Ph.D. Thesis, University of New England, 1981.
(135) Reynolds, P. A.; Figgis, B. N. *Inorg. Chem.* **1991**, *30*, 2300.